The Development of Large-area, Fast, Time-of-Flight Detectors

PROJECT SUMMARY

We propose a program to develop a basic family of economical robust large-area photo-detectors that can be tailored for a wide variety of applications that now use photomultipliers. Advances in materials science and nano-technology, complemented by recent innovations in microelectronics and data processing, give us an opportunity to apply the basic concept of micro-channel plate detectors to the development of large-area economical photo-detectors with quantum efficiencies and gains similar to those of photo-tubes, and with inherent good space and time resolution. The new devices are designed to cover large areas economically, being a sandwich of simple layers rather than an assembly of discrete parts. The plan of R&D that follows is intended to solve the critical technical issues and to deliver proto-types that are ready to be commercialized within 3 years.

The initial use of glass capillary MCP substrates and conventional photo-cathode technology provides a proven solution for each of these components on the critical path. Mechanical assembly and the extension of existing photo-cathode technology to large area planar applications, while formidable tasks, are within the scope of current industrial practice. We have the capabilities and facilities at Argonne, the Space Sciences Laboratory (SSL), and our industrial partners to extend the known technologies.

We have also identified three areas in which new technologies have the potential for transformational developments. First, the development of higher quantum efficiency photo-cathodes based on nano-science morphology with customized work-functions and the adaptation of techniques from the solar-energy sector would allow large area detectors and possibly cheaper assembly techniques. Second, Atomic Layer Deposition (ALD) provides a powerful technique for control of the chemistry and surface characteristics of new photo-cathodes. ALD also can be used to form the secondary emission surfaces of the channels one molecular layer at a time, including controlling the geometry of the electron cascade itself, to enable functionalization of channel-plate substrates with high gain and low noise. This capability allows the separation of the properties of the substrate material from the amplification functionality. We have experience in self-organized nanoporous ceramic (Anodic Aluminum Oxide, AAO) that would provide low-cost batch-produced substrates, and also are investigating substrates made from glass capillaries. Lastly, we have already demonstrated that fast waveform sampling using CMOS ASICs at both ends of transmission line anodes allows the coverage of large areas with small numbers of channels, permitting excellent time and space resolution and a built-in noise identification and reduction mechanism. Design work has started on an ASIC with 2-4 times the number of channels per chip than present chips.

Large-area, robust, and affordable photo-detectors would be transformational in a wide variety of areas. Possible applications include cheaper and more precise Positron Emission Tomography (PET) cameras in medical imaging, scanners for transportation security, and particle detectors in high-energy neutrino and collider physics, astrophysics, and nuclear physics. There would also be many possibilities for new products and spin-off technologies. Because the new devices are planar, relatively thin, and physically robust, they will require less volume and infrastructure in large-area applications for which photomultipliers are presently the current solution, providing additional economies and offering new measurement opportunities.

To meet the challenges we have assembled an experienced cross-disciplinary team that integrates expertise and facilities of national laboratories, universities, and industry, and that includes expertise in both the basic and the applied sciences.

a stand-alone module of a typical size for collider or medical imaging applications, and a large panel for low-rate large-area applications. A brief summary and acknowledgments are given in Sections 5 and 6, respectively.

The work plans for each of the sub-areas of development are described in Section 7. Section 8 describes the management structure. The milestones, organized by task and effort, are presented in Section 9. The budget for each of the three years is presented in Section 10, and Section 11 contains the budget justification.

Appendix A describes several applications for which large-area photo-detectors with good space and time resolution would be transformational. Additional detail on the front-end electronics, photo-cathodes, MCP substrates, and Atomic Layer Deposition is given in Appendices B-E. Lastly, biographical sketches are presented in Appendix F.

2 The Critical-Path to Large-Area Fast Detectors: the Needed Three Developments

We see three areas in which our expertise can be applied to develop economical large-area MCP-PMT 's. They are: 1) the scale-up and modification of photo-cathode production technology for larger area planar devices; 2) implementing solutions to the 'first-strike' problem of developing substrates that satisfy the geometry for channel-plate amplification, are low cost and scalable to large areas, and that may also allow new geometries with higher photon detection efficiency and improved single photo-electron resolution; and 3) solving the time/amplitude/transverse-size complementarity problem. We have spent the last several years solving the third problem, and the solution, transmission-line anodes to preserve the signal amplitude and shape with cheap fast low-power waveform sampling on both ends, is the breakthrough that enables the creation of large-area photo-detectors[37, 24].

We bring to these efforts the resources of the Advanced Photon Source (APS), the Center for Nanoscale Materials (CNM), and the Electron Microscopy Center (EMC) at Argonne, as well as the expertise in the five Divisions. Each of the other institutions in the collaboration brings extensive experience in one of the three critical areas, with decades of experience with photo-cathodes at SSL, industrial expertise represented by Arradiance in emissive materials, Muons,Inc in MCP-PMT simulation, and Synkera in self-organized nanoporous ceramics, and long and successful track records by Chicago, Hawaii, and Argonne in electronics systems.

2.1 Photo-cathodes

2.1.1 Conventional Bialkali Photo-cathodes

There have been major advances in photo-cathode development in recent years [1]. Figure 3 shows the recent gains in quantum efficiency by Hamamatsu versus wavelength (left-hand panel), as well as the spectrum of Cherenkov light as observed through water [39] as a reference input spectrum. The technique is very advanced, giving QE of over 40% in the UV/visible spectral regions today. In addition, photocathode processing is low cost and has good yields [36].

We plan to use conventional bialkali photo-cathodes in an $8'' \times 8''$ format and a conventional transmission geometry as the primary choice. SSL has a long history of successfully producing photo-cathodes [40, 41, 42]. The SSL group has produced conventional photo-cathodes larger than 5" square,and has the facilities to go to 8" square, the size we are considering as our basic sub-assembly. The 8" size will also fit in process equipment routinely used by the semi-conductor industry.

The strategy for the bialkali photo-cathodes will be to optimize the SSL bialkali quantum efficiences on development-size (32.8mm) window samples to increase the present quantum-efficiency from $\sim$20% to 30% or more in small samples, and to achieve uniformity in large samples. Once we have achieved the required quantum-efficiency, we will extend the process to the $8'' \times 8''$ format. Work will continue in collaboration with the materials science efforts at Argonne in characterization and simulation, to improve the quantum-efficiency beyond 30%, which is now routinely available from industry(See Figure 3).

We will also explore the quantum-efficiency and stability of opaque photo-cathode geometries by putting cathodes directly on ALD treated substrates in the 32.8 mm development format (see Section 2.2. In principle, opaque photo-cathodes combined with anti-reflection coatings and photon internal capture techniques developed by the solar cell industry should give an increase in quantum-efficiency [43].

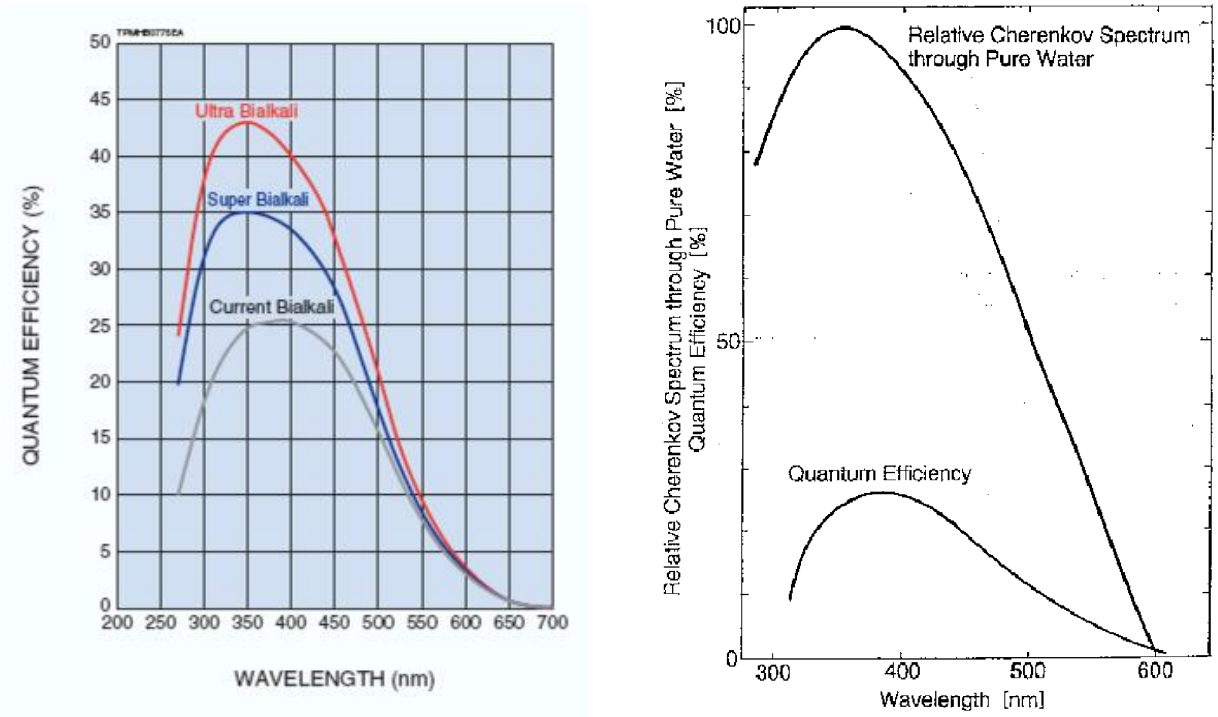

Figure 3: Left: Quantum efficiencies for Hamamatsu bialkali photocathodes, showing the recent developments. Right:The spectrum of Cherenkov light in water, and the quantum efficiency of the Hamamatsu 20" photo-tube used in Super-K (from Ref. [39])

2.1.2 R&D on Nano-scale Photo-cathodes

In parallel with getting our bialkali quantum-efficiency up to industry standards, we will devote effort to develop advanced photo-cathodes using the facilities and strengths in nano-materials at Argonne. The effort will share characterization and test facilities, standard substrates, standard measurement criteria, and expertise with the mainstream effort on bialkali photo-cathodes. The effort will be a coordinated effort between the Advanced Photon Source, Materials Science, Energy Systems, Math and Computer Science, and High Energy Physics Divisions at Argonne and which will take advantage of unique user facilities at the Argonne Advanced Photon Source (APS), Center for Nanoscale Materials (CNM), and Electron Microscopy Center (EMC). In particular, our goal is to develop novel photo-cathodes that appear 'black' to photons in the required spectral region, have high electron emissivity, and can be applied to large panels using Atomic Layer Deposition (ALD) or Chemical Vapor Deposition (CVD), as briefly described below and in Appendix C. A list of references is also attached to Appendix C.

The development of a radically new photocathode material based on nano-technology has the potential for comparable or higher quantum efficiencies (QE's) by optimizing the cathode surface morphology and dielectric constant, and thus tailoring the near-surface electric field so that it significantly enhances photo-electron emission. This approach can become an alternative to lowering the surface work-function of a conventional photo-cathode by fine (and expensive) tuning of its already complex chemical composition. Additional gains in overall detector efficiency may be obtained by using nano-engineered photon-trapping surface geometries with reduced reflection losses, thus benefiting from technologies now standard in the solar cell industry.

The goal for higher quantum efficiency using nano-technology is based on evading the fundamental limitations of conventional transmission photo-cathodes, which are that the electron escape depth is typically smaller than the photon absorption length. This leads to low photon-to-electron conversion eficiency, high energy spread, and a wide angular distribution. Using nano-technology one can optimize the surface technology as shown in Figure 4. What is attractive about nano-technology is that various methods exist to grow different morphologies so that there is a wide range of possibilities(See Figure 5). It is relatively cheap and scalable to large production quantities, and is inherently industrially compatible. Electronic properties can be widely manipulated. However electronic properties and structure are strongly dependent on specific growth conditions, and the basic understanding is not yet solid. A development program thus must have the ability for rapid throughput for

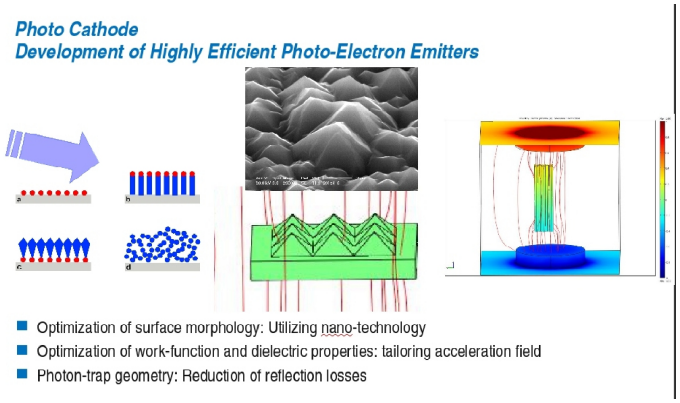

Figure 4: Some basic ideas for developing highly efficient cathodes [44]: using non-normal incidence, back reflectors, total internal reflection, tuning of feature size to minimize reflection and maximize absorption, and control of secondary emission by morphology.

testing many different parameters in parallel, facilities for hard-science characterization and measurement, and theoretical and simulation expertise for rational design. All of these have been developed in other contexts at Argonne, and the leaders of these programs have joined forces in the present effort.

Reproducible material synthesis is impossible without accurate characterization. Emission of photo- and secondary electrons is extremely sensitive to materials properties such as surface composition and structure, including contamination and aging. For characterization we will need structural and electronic probes, an automated fast test capability, local probes for work-function measurements, and the ability to make timing and emission angle measurements. For simulation we will need both static and dynamical models and band-structure calculations. We have access to the Center for Nanoscale Materials at Argonne for initial production.

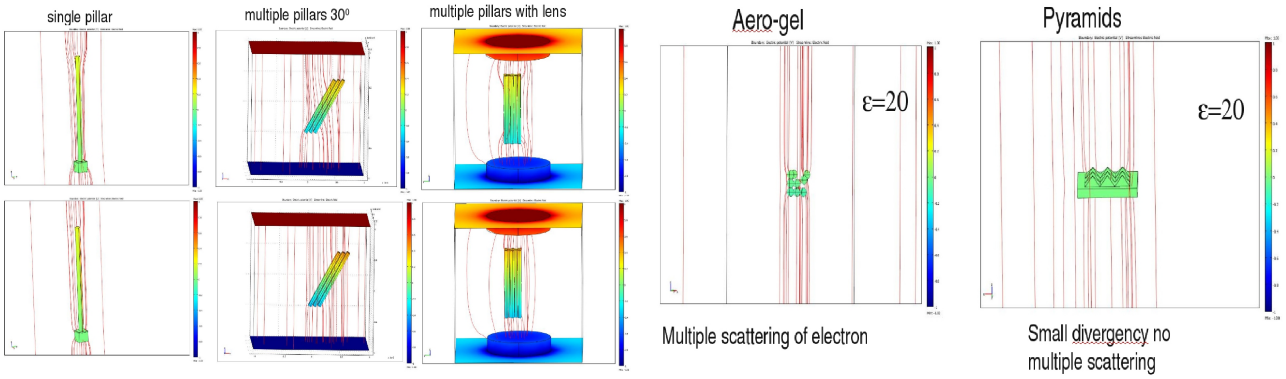

Figure 5: Examples of effects caused by morphology, from a simulation including both the emission characteristics (work-potential- chemistry) and electron optics, including dynamic effects (nano-technology and static/RF-electron simulation). The left-hand panel shows simulations of several geometries; the right-hand panel shows simulations of aerogel and surface pyramid morphologies.

2.1.3 Characterization Facilities

There are programs already underway at Argonne in the APS and HEP Divisions on the development of high-performance photo-cathodes. The authors of the present proposal include experts on the physics of photo-cathodes, the material fabrication and processing of the photo-cathodes, surface and material properties of the photocathode using various techniques such as x-ray diffraction and photo-emission, and the characterization of the photoelectrons generated from these photo-cathodes, such as the distributions in energy and angle. This will allow us to apply the revolution in surface chemistry due to the application of sophisticated surface analysis facilities and theoretical knowledge implemented in simulations to large-area MCP-PMT 's.

We are uniquely able to perform advanced characterization of efficiency vs composition using several highly-evolved facilities at Argonne. Figures 6 and 7 provide a succinct description of the facilities for sputter-depth profiling and sample volatilization, electron-microscope mapping, and nanometer-scale analysis.

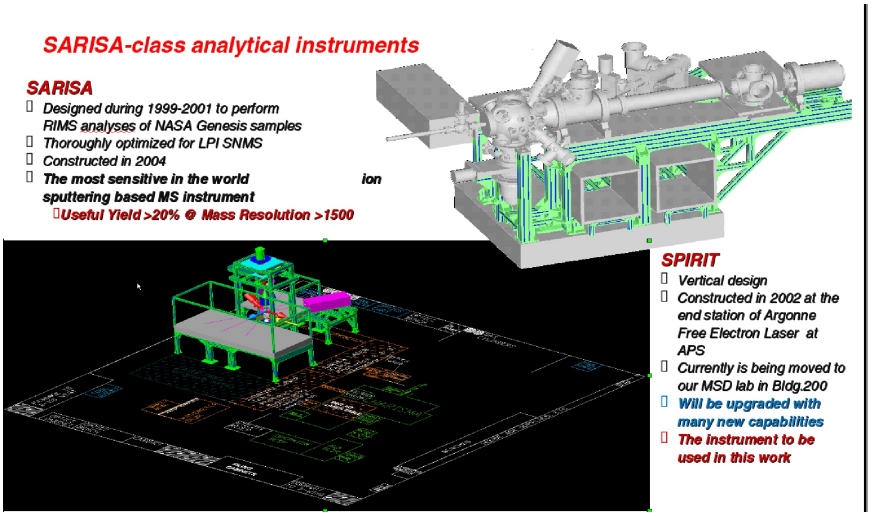

Figure 6: The SARISA-class instruments to be used for characterization and testing of photo-cathode and electron-emitting materials (from I. Veryovkin [45]).

2.2 The First Strike Problem

2.2.1 Introduction to Amplification in Micro-Channels

The second problem on the critical path is to make arrays of channels that have the required characteristics for high efficiency and gain, low noise, a good transit-time-spread, and good amplitude resolution for single photo-electrons. These characteristics include providing a well-defined surface for the first-strike for the incoming photo-electron, large open-area-ratios, and an interior surface with electrical and physical properties to sustain a cascade with enough gain and current capability, while maintaining an acceptable dark current.

We have strength and experience in the technologies needed to attack these problems at Argonne, Arradiance, SSL, and Synkera. Many of the problems have been studied by members of our team [46, 47, 48, 49,

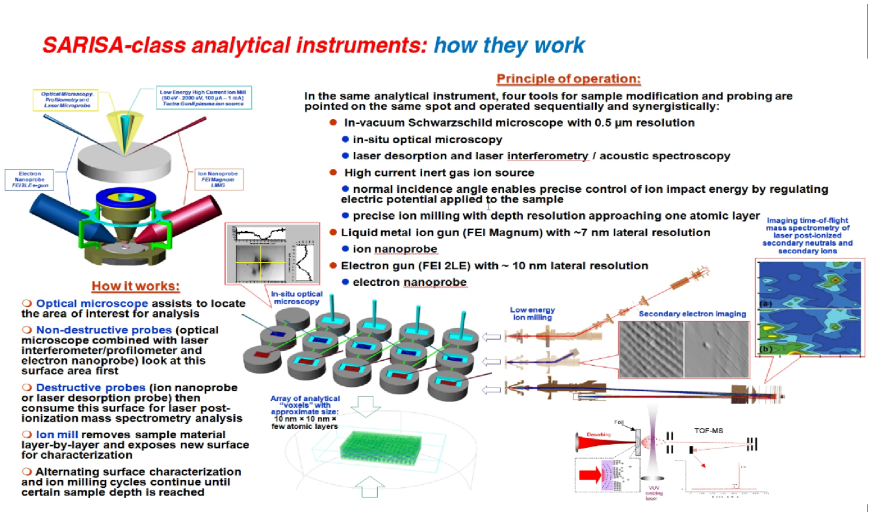

Figure 7: An explanation of how the SARISA-class instruments work (from I. Veryovkin [45]).

7.6 Amplification Stage: Substrates, Coatings, Scaling

The adaptation of capillary-based glass substrates from industry is being coordinated through Argonne and Chicago. In parallel, the development of AAO substrates with funnel geometries will be a joint effort of Argonne, SSL, and Synkera. The ALD development for the substrate resistive and emissive coatings is the responsibility of Argonne, in collaboration with Arradiance and Synkera.

7.7 Anode

The basic R&D for the anode has been done in the last several years by a collaboration of Chicago, Argonne, and Fermilab. Extending this to larger areas, including possibly using glass as a cheaper substrate, will be done by the same group, in close consultation with the experts at SSL. RF simulations of the anode that have been developed at Chicago, and that agree very well with measurements made with the Argonne laser test stand [67], will be used to design and validate new anode designs.

7.8 Front-End Electronics

The front-end wave-form sampling electronics is relatively advanced based on the work at Chicago, Hawaii, Orsay, PSI, Saclay, and SLAC. Work has started at Chicago and Hawaii to move the design of the waveform sampling chip to the more modern 130 nm IBM CMOS process that will support up to 32 channels per chip. The development of the FPGA-based control and DAQ system will be done at Argonne, Chicago, and SSL. The clock distribution system work will be also done at Argonne in a collaboration of the HEP and APS Divisions.

7.9 Mechanical Assembly

We are pursuing two parallel paths for the mechanical package. The first is the logical extension of widely-used and well-understood ceramic package, with metal-to-ceramic seals. This work will be done at SSL, where there is tooling and extensive experience. A second effort to develop an all-glass mechanical assembly using techniques developed for large flat panel screens is being started at Argonne, Chicago, and Fermilab, with consultation by SSL. As different applications will have different requirements on robustness (the SSL experience in successfully making devices that withstand rocket launchings is one example), required area, and cost, we foresee pursuing both these paths to the completion of a ($8'' \times 8''$) prototype.

7.10 Integration

Integration of these efforts, including managing the budgets, schedule, and reviews, will be the responsibility of Argonne.

8 Management

8.1 Overview

The management of this program will be done through the HEP Division of Argonne.

8.2 Industry/Lab Partnerships

We see the efforts in ALD and AAO as a partnership between the national laboratories and industry. We are in the process of establishing the formal protocols on IP and deliverables, with one NDA in place with Synkera, one being negotiated with Arradiance, and a joint SBIR submitted with Muons,Inc.

8.3 Reviews

We expect regular reviews of the program by the DOE. We will also establish internal review committees ('god-parents' [68]) from inside the collaboration, with outside experts added as needed, with the responsibility to regularly review progress in the individual areas.

8.4 Transparency/Dissemination

We aim for a unified, transparent effort with built-in reviews and documentation. We have already put a structure in place, with a web page (http://hep.uchicago.edu/psec/), a regular weekly meeting, a blog for results and presentations, two broadly-attended workshops per year since 2005 [25], and several formal collaborations and MOU's. We report our work at IEEE, Real-Time, and other technical conferences, with papers in the proceedings [69].

9 Milestones

9.1 Year 1

1. **Photo-cathode Group** *Siegmund,Attenkofer,Insepov,Pellin,Yusof*
   (a) Demonstrate a quantum efficiency $\geq$ 25 % with a bialkali photo-cathode on a solid glass plate, with acceptable dark current;
   (b) Produce a $8'' \times 8''$ conventional photo-cathode with photo-cathode quantum efficiency. $\geq$ 25 %.
   (c) Screen and test flat and morphology-based negative-electron-affinity materials and compare to simulation.

2. **Glass Substrate Group** *Tremsin,Frisch,Siegmund,Hau,Pellin,Sullivan*
   (a) Develop and characterize 32.8mm glass substrates with 10-40 micron pores diameters L/D of 40, a bias angle of 8 degrees, and an open area ratio $\geq$ 80% suitable for an MCP;
   (b) Acquire and test $8'' \times 8''$ plates;
   (c) Evaluate the process economics.

3. **Advanced Substrate Group** *Wang,Routkevitch,Pellin*
   (a) Achieve straight pores in AAO with diameter $\geq$ 0.7 microns (no-funnel option), 40 <L/D< 100, and open-area ratio $\geq$ 60 %;
   (b) Demonstrate the feasibility of making AAO funnels suitable for photo-cathode deposition;
   (c) Produce blanks of 32.8mm AAO plate for tests and MCP development.
   (d) Evaluate the process economics.

4. **Atomic Layer Deposition Group** *Elam,Insepov,Sullivan,Libera,Wang*
   (a) Systematically characterize the leading ALD materials for Photo-emission and Secondary Electron Emission (SEE);
   (b) Demonstrate gain > 1000, non-uniformity to < 25% with ALD on a 32.8mm glass capillary substrate MCP, with acceptable dark current;

5. **Testing Group** *Adams,Veryovkin,Attenkofer,Genat,May,Nishimura,Ramberg, Ronzhin, Va'vra, Varner,Wetstein,Zinovev*
   (a) Set up test protocols for the various test facilities and make appropriate modifications to accomodate up to $8'' \times 8''$ plates.
   (b) With the Simulation Group, set up data-base for systematic codification of test results.
   (c) Expeditiously test the functionalized development units from the ALD and Photo-cathode Groups

6. **Simulation Group** *Ivanov,Beaulieu,Abrams,Genat,Insepov,Roberts,Tremsin,Tang*
   (a) With the Test Group, set up data-base for systematic codification of test results.
   (b) Systematically compile existing data on materials and define the needed measurements for characterization by the Emissive Materials Group;
   (c) Complete the MCP simulation code including space charge;
   (d) Validate the simulation with commercial tubes;
   (e) Complete a first-generation glass-substrate-based MCP-PMT simulation;
   (f) Complete a first-generation AAO/ALD-based MCP-PMT simulation;
   (g) Optimize funnel and pore shapes for an MCP-PMT with opaque photo-cathode.

7. **Mechanical Assembly Group** *Stanek,Northrop,Anderson,Forbush,Genat,Ronzhin,Sellberg,Siegmund, Tremsin,Wetstein,Zhao*
   (a) Identify candidate materials, vendors, and construction methods for the $8'' \times 8''$ and $4' \times 2'$ modules;
   (b) Complete an initial mechanical/electrical design for proto-type glass and ceramic $8'' \times 8''$ modules, and construct mechanical proto-types (no photo-cathode yet);
   (c) Measure the vacuum, residual gases, out-gassing rates, and surface chemistry of proto-type modules;
   (d) Assemble a complete Development(32.8mm) AAO/ALD or glass capillary MCP-PMT with conventional photo-cathode for testing.
   (e) Evaluate the process economics.

8. **Electronics Group** *Varner,Genat,Anderson,Bogdan,Drake,Frisch,Heintz,Kennedy, Nishimura,Rosen,Ruckman,Tang*
   (a) Construct and test a $8'' \times 8''$ proto-type transmission-line anode (e.g. velocity, time resolution, cross-talk, attenuation);
   (b) Construct a first-generation clock distribution system;
   (c) Construct a first-generation DAQ system;
   (d) Construct a first-generation anode PC card with existing sampling chips [23, 22];
   (e) Submit a first IBM-8RF chip with timing control, sampling capacitor chain, and ADC blocks.
9. **Integration Group** *Drake,Genat,Anderson,Byrum,Frisch,Ronzhin,Sanchez,Siegmund,Tremsin,Wetstein*
   (a) Install the first-generation clock distribution system and DAQ computer in the integration area;
   (b) Integrate the first-generation DAQ and MCP with first-generation front-end card with existing sampling chips;
   (c) Integrate the individual tests into a user-accessible system suite.
10. **Management Group** *Frisch,Siegmund,Byrum,Pellin,Weerts*
   (a) Identify the senior staff member at Argonne responsible for tracking costs, schedules, responsibilities, and reviews;
   (b) Identify co-leaders for each of the groups.
   (c) Establish the project in the appropriate project manager software;
   (d) Establish preliminary major decision points for photo-cathode, geometry, substrate, module size, mechanical assembly, and cost;
   (e) Select internal review committees and schedule reviews;
   (f) Survey and clarify IP and future production relationships with industry;
   (g) Evaluate the process economics for each major component.

9.2 Year 2

1. **Photo-cathode Group** *Siegmund,Attenkofer,Insepov,Pellin,Yusof*
   (a) Construct a facility for production and vacuum transfer of $8'' \times 8''$ conventional (bialkali) photo-cathodes with quantum-efficiency $\geq 25\%$.
   (b) Demonstrate advanced photo-cathode quantum efficiency >35%;
   (c) Continue and refine the development and characterization of novel materials for Photo-emission and Secondary Electron Emission (SEE): Higher quantum efficiency (QE), nano-structures, photon trapping usingwavelength tuning;
2. **Glass Substrate Group** *Tremsin,Frisch,Siegmund,Hau,Pellin,Sullivan*
   (a) Achieve open-area ratios $\geq 80\%$ and channel sizes ≤ 20 microns;
   (b) Optimize the process economics for large areas.
3. **Advanced Substrate Group** *Wang,Routkevitch,Pellin*
   (a) Achieve straight pores with diameter $\geq$1 micron, $40 \leq$ L/D$\leq$100, and open-area ratio $\geq$70% (no-funnel option) or $\geq$90% (funnel option)"
   (b) Demonstrate gain > 1000, non-uniformity to < 15% in an advanced plate.
   (c) Perform initial scale-up and develop cost projections for 8"x8" AAO with large pores.
4. **Atomic Layer Deposition Group** *Elam,Sullivan,Insepov,Libera,Wang*
   (a) Demonstrate gain > 1000, non-uniformity to < 15%
   (b) Optimize process economics for batch production
   (c) Develop multi-dynode stripe coating of channel SEE layers for narrowing gain and transit-time spreads;
5. **Testing Group** *Adams,Veryovkin,Attenkofer,Genat,May,Nishimura,Ramberg, Ronzhin,Va'vra, Varner,Wetstein,Zinovev*
   (a) Expeditiously test the functionalized development units from the ALD and Photo-cathode Groups
   (b) Set up to test completed MCP-PMT 's in development and $8'' \times 8''$ sizes in the Argonne laser test-stand and MTEST.
6. **Simulation Group** *Ivanov,Beaulieu,Abrams,Genat,Insepov,Roberts,Tremsin,Tang*
   (a) Validate simulation of morphology-based emissive materials
   (b) Include dynamic effects in MCP simulation
   (c) Completion of 'end-to-end' simulation package.
7. **Mechanical Assembly Group** *Stanek,Northrop,Anderson,Forbush,Genat,Ronzhin,Sellberg,Siegmund, Tremsin,Wetstein,Zhao*
   (a) Construct working glass and ceramic $8'' \times 8''$ MCP-PMT 's with gain $\geq 5 \times 10^5$
   (b) Finish design of $4' \times 2'$ module.
8. **Electronics Group** *Varner,Genat,Anderson,Bogdan,Drake,Frisch,Heintz,Kennedy, Nishimura,Rosen,Ruckman,Tang*
   (a) Construct and test 4-foot PC card with Varner and Ritt chips
   (b) Construct clock distribution system for MTEST test-beam
   (c) Construct DAQ system for MTEST test-beam
   (d) Construct second-generation front-end card for MTEST test-beam
   (e) Submit second IBM-8RF chip (4-channel)
9. **Integration Group** *Drake,Genat,Anderson,Byrum,Frisch,Ronzhin,Sanchez,Siegmund,Tremsin,Wetstein*
   (a) Integrate first-generation DAQ and $8'' \times 8''$ MCP with anode and front-end
   (b) Continue development of system test suite
10. **Management Group** *Frisch,Siegmund,Byrum,Pellin,Weerts*
    (a) Review of Progress
    (b) Review of Major Decision Points on Photo-cathode, Substrate, Module Size, Assembly, and Cost
    (c) Re-evaluate process economics for each component
    (d) Get another Program Director

9.3 Year 3

1. **Photo-cathode Group** *Siegmund,Attenkofer,Insepov,Pellin,Yusof*
   (a) Produce a $8'' \times 8''$ conventional photo-cathode with photo-cathode quantum efficiency. ≥ 35 % with acceptable dark current;
   (b) Continue the characterization survey of novel materials for Photo-emission and Secondary Electron Emission: higher quantum efficiency , nano-structures, wavelength tuning.

2. **Glass Substrate Group** *Tremsin,Frisch,Siegmund,Hau,Pellin,Sullivan*
   (a) Evaluate the process economics for large-area, psec timing, and medical applications.
   (b) Setup for industrial-scale production of plates optimized for the ALD coating process and robust mechanical assembly;

3. **Advanced Substrate Group** *Wang,Routkevitch,Pellin*
   (a) Evaluate the process economics for large-area, psec timing, and medical applications.
   (b) Fabricate scaled substrates in quantities and sizes sufficient for 6 working proto-type modules;
   (c) Continue exploring advanced processes and pore geometries for cheaper production and higher QE.

4. **Atomic Layer Deposition Group** *Elam,Sullivan,Insepov,Libera,Wang*
   (a) Evaluate the process economics for large-area, psec timing, and medical applications.
   (b) Achieve single-photo-electron resolution out to 4 pe's.
   (c) Continue the characterization survey of novel materials for Photo-emission and Secondary Electron Emission: higher quantum efficiency , nano-structures, wavelength tuning.

5. **Testing Group** *Adams,Veryovkin,Attenkofer,Genat,May,Nishimura,Ramberg, Ronzhin,Va'vra, Varner,Wetstein,Zinovev*
   (a) Transition to industrial-style testing.
   (b) Continue to test innovations on a small scale.

6. **Simulation Group** *Ivanov,Beaulieu,Abrams,Genat,Insepov,Roberts,Tremsin,Tang*
   (a) Continue development of codes for field-emission-based photo-cathode and secondary emission materials.

7. **Mechanical Assembly Group** *Stanek,Northrop,Anderson,Forbush,Genat,Ronzhin,Sellberg,Siegmund, Tremsin,Wetstein,Zhao*
   (a) Build a quantity of $8'' \times 8''$ and $4' \times 2'$ modules; [10]
   (b) Design and optimize quantity assembly procedures;
   (c) Continue to interface to applications through Psec Workshop Series [25] and mutual collaborators.

8. **Electronics Group** *Varner,Genat,Anderson,Bogdan,Drake,Frisch,Heintz, Kennedy,Nishimura,Rosen,Ruckman,Tang*
   (a) Design production generation clock distribution;
   (b) Design production FPGA DAQ/control card;
   (c) Submit 16(32)- channel IBM-8RF chip.

9. **Integration Group** *Drake,Genat,Anderson,Byrum,Frisch,Ronzhin,Sanchez,Siegmund,Tremsin,Wetstein*
   (a) Assemble a 4-module system;
   (b) Test 4-module system.

10. **Management Group** *Frisch,Siegmund,Byrum,Pellin,Weerts*
    (a) Establish production hand-off of modules to industry;
    (b) Establish paths to application-specific modifications of the generic devices;
    (c) Set up a lab/industry/university group charged with exploring other applications and transformational developments.

[10] Enough to establish quality control, uniformity, and enough to use in preliminary applications.

11 Budget Justification

References

[1] The Hamamatsu Ultra Bialkali photo-cathode has achieved a quantum efficiency of 43%. See http://jp.hamamatsu.com/resources/products/etd/eng/html/pmt_003.html

[2] For example, the Hamamatsu R9800 25-mm tube has a transit time spread (TTS) of 270 psec (FWHM). See www.hamamatsu.com.

[3] For example, see http://sales.hamamatsu.com/multianode/

[4] K. Arisaka et al., "Performance of a Prototype Aerogel Counter Readout", http://www.scientificcommons.org/40872582 (2008)

[5] Arisaka, K. et al., "XAX: a multi-ton, multi-target detection system for dark matter, double beta decay and pp solar neutrinos", ArXiv http://arxiv.org/abs/0808.3968 (2008)

[6] Photonis/Burle Industries, 1000 New Holland Ave., Lancaster PA, 17601. See http://www.photonis.com/industryscience/products/microchannel_plates_detectors/reference_list

[7] See http://sales.hamamatsu.com/en/products/electron-tube-division/detectors/microchannel-plates-mcps.php

[8] See http://www.photek.com/

[9] O.H.W. Siegmund, Barry Welsh, John Vallerga, Anton Tremsin, Jason McPhate, "High-performance microchannel plate imaging photon counters for spaceborne sensing", Proc. SPIE Vol. 6220 (2006) 622004

[10] Siegmund, O.; Vallerga, J.; Jelinsky, P.; Michalet, X.; Weiss, S.; Cross delay line detectors for high time resolution astronomical polarimetry and biological fluorescence imaging, Nuclear Science Symposium, 2005 IEEE, Volume 1, 23-29 Oct. 2005 Page(s):448 - 452

[11] P. Jelinsky, P. Morrissey, J. Malloy, S. Jelinsky, and O. Siegmund, C. Martin, D. Schiminovich, K. Forster, T. Wyder and P. Friedman, Performance Results of the GALEX cross delay line detectors, Proc. SPIE Vol. 4854, pp 233-240, 2003.

[12] In addition to the above references, see: O.H.W. Siegmund, John Vallerga, Anton Tremsin, Characterizations of microchannel plate quantum efficiency, Proc. SPIE Vol. 5898 (2005) 58980H.

[13] O. H. W. Siegmund, A. S. Tremsin, C. P. Beetz, Jr., R. W. Boerstler, D. R. Winn, "Progress on development of silicon microchannel plates", SPIE Proc., vol. 4497, 139-148, 2002.

[14] A.S. Tremsin, O.H.W. Siegmund, C.P. Beetz R.W. Boerstler, The latest developments of high gain Si microchannel plates. Proc. SPIE Vol. 4854, pp 215-224, 2003.

[15] High amplitude events in microchannel plates, O.H.W. Siegmund, J. Vallerga, and P. Lammert, IEEE Trans. Nucl. Sci., NS-36, 830-835 (1989).

[16] V. Ivanov, Computation Methods and Device Optimization in Electron Optics (2 volumes, in Russian), Moscow, 2005.

[17] See http://www.arradiance.com/, including a A. S. Tremsin, H. F. Lockwood, D. R. Beaulieu, N. T. Sullivan, E. Munro, J. Rouse, "3D microscopic model of electron amplification in microchannel amplifiers for maskless lithography", 7th International Conference on Charged Particle Optics, Cambridge, England, July 2006, Physics Procedia 1 (2008) 565.

[18] A.B. Berkin, V.V. Vasilyev, "Numerical simulation of the amplification regime for pulsed current in the channel of MCP", June 2007 (in Russian); A.B. Berkin, V.V. Vasilyev, "Numerical model of the amplification regime for the direct current in the channel of MCP", June 2007 (in Russian); A.J. Guest, "A computer model of channel multiplier plate performance", 1971

[19] J. Milnes and J. Howorth, (Photek Ltd.), "Picosecond Time Response Characteristics of Micro-channel Plate PMT Detectors"; SPIE USE V.8, 5880 (2004); "Advances in Time Response Characteristics of Micro-channel Plates", http:/www.photek.com/support/technical_papers.htm

[20] D. Breton, E. Auge, E. Delagnes, J. Parsons, W Sippach, V. Tocut, The HAMAC rad-hard Switched Capacitor Array. ATLAS note. October 2001. Breton

[21] E. Delagnes, Y. Degerli, P. Goret, P. Nayman, F. Toussenel, and P. Vincent. SAM : A new GHz sampling ASIC for the HESS-II Front-End. Cerenkov 2005

[22] S. Ritt. "The DRS chip: Cheap waveform digitizing in the GHz range."; Nucl.Instrum.Meth.A518:470-471,2004

[23] G. Varner, L.L. Ruckman, J.W. Nam, R.J. Nichol, J. Cao, P.W. Gorham, and M. Wilcox. The Large Analog Bandwidth Recorder And Digitizer with Ordered Readout (LABRADOR) ASIC, Nucl.Instrum.Meth.A583:447-460,2007.

[24] J.-F. Genat, G. Varner, F. Tang, H. Frisch; "Signal Processing for Pico-second Resolution Timing Measurements",To be published in Nucl. Instr. Meth., 2009; arXiv:0810.5590. We have noticed in our discussions with groups interested in applications that our natural translation of time resolution into space resolution along the distance of travel is not commonly shared; it takes some getting used to for the words 'time resolution of 10 psec' to naturally represent a resolution of 3 mm (or less if in a medium) in the direction the photon or charged particle came from.

[25] For the agendas and slides of the last 7 workshops, see http://psec.uchicago.edu/workshops.php

[26] Q. Xie, C.-M. Kao, X. Wang, N. Guo, C. Zhu, H. Frisch, W.W. Moses, C.-T. Chen; " Potential Advantages of Digitally Sampling Scintillation Pulses in Timing Determination in PET", Nuclear Science Symposium Conference Record, 2007. NSS '07; Vol. 6: 4271-4274

[27] H. Kim C.-M. Kao, Q. Xie, H. Frisch, W. W. Moses, W.-S. Choong, L. Zhou, F. Tang, J. Lin, O. Biris, and C.-T. Chen; "A Multi-Threshold Method for TOF-PET Signal Processing". Nucl. Instrum. Meth. A 602, 618-621(2009)

[28] D. Herbst, " Time of Flight in PET Using Fast Timing and Leading Edge Fit Optimization", Submitted to IEEE08, October, 2008; Dresden Germany

[29] J. Lin, O. Biris, C.-T. Chen, W.-S. Choong, H. Frisch, C.-. Kao, W. W. Moses, F. Tang, Q. Xie, L. Zhou; "Electronics development for fast-timing PET detectors: The multi-threshold discriminator Time of Flight PET system", Proceedings of SORMA, Berkeley CA, May, 2008.

[30] Q. Xie, C.-M. Kao, X. Wang, N. Guo, C. Zhu, H. Frisch, W.W. Moses, C.T. Chen;
"Potential Advantages of Digitally Sampling Scintillation Pulses in Time Determination in PET", NSSC/MIC IEEE, Honolulu, Hawaii, Oct 27-Nov 3, 2007.

[31] H. Nicholson, private communication. We are also grateful for the strong push toward developing much larger detector modules than we had envisioned.

[32] The surface area of the solenoidal magnet coil cryostats for both ATLAS and CDF is close to 30 m^2. The idea is to 'tile' the outside of the solenoidal coil, where magnetic fields are not a problem. We have performed simulations that show that interactions in the coil are not a problem for charged particles. The coil also can serve as a 'pre-converter' for photons, for which the system should provide excellent time (i.e. space) resolution.

[33] We thank Neville Harnew for guidance on the LHCb requirements. A typical design for an LHCb upgrade is a coverage of 5m x 6m (of order 10 m from the interaction point) to achieve charged-particle (K/pi) identification in the 1-10 GeV range. The system easily fits in the available longitudinal length of 30 cm.

[34] William Moses (LBNL), private communication. We thank Dr. Moses for also providing us with a rough cost estimate for a typical system.

[35] Patricia Dehmer, Deputy Director for Science Programs, DOE Office of Science, HEPAP, Feb. 2009, as quoted by H. Nicholson, The Development of Large Area Psec Photo-Devices; Workshop VII, Argonne National Laboratory, Lemont, IL; 26-27 February 2009; http://psec.uchicago.edu/workshops.php

[36] We thank Paul Hink (Photonis) for influential input to this section.

[37] Henry J. Frisch, Harold Sanders, Fukun Tang, and Tim Credo; United States Patent 7485872, "Large area, pico-second resolution, time of flight detectors".

[38] See, for just one example, http://www.industrial-lasers.com/display_article/330518/39/none/none/eat/Laser-glass-cutting-in-flat-panel-display-production. We have initiated contacts with a number of firms in the industry, and also have dedicated glass expertise on the staff at Argonne. We have started design work at Argonne and Chicago on the details of a glass solution, including the best way to connect to the HV and signals. What is shown is just a 'cartoon' illustrating the basic ideas.

[39] Masaki Ishitsuka, "L/E analysis of the atmospheric neutrino data from Super-Kamiokande"; Ph.D Thesis, University of Tokyo, Feb., 2004

[40] O. Siegmund, J. Vallerga, J. McPhate, J. Malloy, A. Tremsin, A. Martin, M. Ulmer and B. Wessels, Development of GaN photocathodes for UV detectors, Nuclear Instruments and Methods in Physics Research Section A: Vol. 567, Issue 1, 2006, Pages 89-92

[41] A.S. Tremsin, O.H.W. Siegmund, Quantum efficiency and stability of alkali halide UV photocathodes in the presence of electric field, Nuclear Instruments and Methods in Physics Research (sect. A), Vol. 504 (2003), 4-8.

[42] A.S. Tremsin and O.H.W. Siegmund, Polycrystalline diamond films as prospective UV photocathodes, Proc. SPIE, 4139, 16, (2000)

[43] Hellmut Fritszche, private communication.

[44] K. Attenkofer, talk Workshop on the Development of Large Area Psec Photo-Devices; Workshop VII, Argonne National Laboratory, Lemont, IL; Feb. 2009; http://hep.uchicago.edu/psec/

[45] I. Veryovkin, talk Workshop on the Development of Large Area Psec Photo-Devices; Workshop VII, Argonne National Laboratory, Lemont, IL; Feb. 2009; http://hep.uchicago.edu/psec/

[46] See http://www.arradiance.com/, including a link to: D. R. Beaulieu, D. Gorelikov, P. de Rouffignac, K. Saadatmand, K. Stenton, N. Sullivan, A. S. Tremsin; "Nano-engineered ultra high gain microchannel plates"

[47] J.W. Elam, G. Xiong, C.Y. Han, HH Want, J.P. Birrell, U. Welp, J.N. Hyrn, M.J. Pellin, T.F. Baumann, J.F. Poco, and J.H. Satcher, "Atomic Layer Deposition for the Conformal Coating of Nanoporous Materials", Journal of Nanomaterials, 2006, p. 1-5

[48] J.W. Elam, J. A. Libera, M.J. Pellin, and P.C. Stair, "Spatially Controlled Atomic Layer Deposition in Porous Materials", Applied Physics Letters, 2007 **91** (24)

[49] A. M. Dabiran, A. M. Wowchak, P. P. Chow, O. H.W. Siegmund, J. S. Hull, J. Malloy, A. S. Tremsin, "Direct deposition of GaN-based photocathodes on microchannel plates", Proc. SPIE, vol. 7212-38 "Optical Components and Materials VI", San Jose, CA January 2009.

[50] J.W. Elam, D. Routkevitch, S. M. George, "Properties of ZnO/Al_2O_3 Allow Films Grown Using Atomic La;yer Deposition Techniques, J. of the Electrochem. Soc 2003 150(6) G339

[51] A.B.F., J.W. Elam, J.T. Hupp, and M.J. Pellin, "ZnO Nanotube-Based Dye-Sensitized Solar Cells", Nano Letters, 2007(7), P.2183

[52] See http://www.synkera.com, including the links to "Self-organized Anodic Aluminum Oxide" and "Ceramic MEMS" sections.

[53] J. W. Elam, D. Routkevitch, P. Mardilovich, S. M. George, "Conformal Coating of Ultra-high Aspect Ratio Nanopores of Anodic Alumina by Atomic Layer Deposition"; Chem. Materials, 15 (2003) 3507-3517.

[54] This is the term used to describe the coating of the substrate with emittive materials to provide amplification.

[55] The direction of the field lines in the channel is a function of the bulk and surface resistances, and has been the subject of some controversy. In the devices we consider here the lines are parallel to the channel axis provided one is more than several channel diameters away from the ends.

[56] 'Trust but validate', R. R. Reagan, on signing the 1987 Intermediate Nuclear Forces treaty. (http://www.usemod.com/cgi-bin/mb.pl?TrustButVerify).

[57] A. Tremsin, private communication.

[58] Incom,Inc. Charlton Mass. http://www.incomusa.com/

[59] We thank Michael Minot (Incom) and Joseph Renaud from Incom,Inc for the pictures and information.

[60] K. Inami, Workshop on Timing Detectors, Institute of Nuclear Physics in Lyon (IPNL) France, Oct. 2008

[61] J. Va'vra, D.W.G.S Leith, B. Ratcliff, E. Ramberg, M. Albrow, A. Ronzhin, C. Ertley, T. Natoli, E. May, and K. Byrum, submitted to Nucl. Instr. & Meth., March 2009

[62] Hamann, T. W., A. B. F. Martinson, et al. (2008). "Atomic Layer Deposition of TiO2 on Aerogel Templates for Novel Photoanodes in Dye-Sensitized Solar Cells." Journal of Physical Chemistry C 112(27): 10303-10307.

[63] Hamann, T. W., A. B. F. Martinson, et al. (2008). "Aerogel Templated ZnO Dye-Sensitized Solar Cells." Advanced Materials 20(8): 1560-1564.

[64] O.H.W. Siegmund, private communication.

[65] B. W. Adams, K. Attenkofer, Rev. Sci. Instrum. 79, 023102 (2008)

[66] See http://www.arradiance.com/.

[67] K. Byrum, H. J. Frisch, J.-F. Genat, E. May, T. Natoli, F. Tang, "Pico-second Timing with Micro-Channel Plate Devices and Waveform Sampling Readout Electronics", submitted to Real Time 2009, Bejing, China, May 2009.

[68] The large and complex CDF detector at Fermilab was built by subgroups each with its own internal hardware 'god-parent' committee formed of experts from within the collaboration, and chaired by a senior member experienced in that area. These committees averted several major disasters and initiated several major innovations.

[69] F. Tang, C. Ertley, H. Frisch, J.-F. Genat; "Transmission-Line Readout with Good Time and Space Resolution for Large-Area MCP-PMTs", TWEPP, Naxos, Greece (2008); C. Ertley, "Development of Pico-second Resolution Large-Area Time of Flight Systems", SORMA West 2008, Berkeley CA, Poster 136, May 12, 2008; T. Credo, H. Frisch, H. Sanders, R. Schroll, and F. Tang; Proceedings of the IEEE, Rome, Italy, Oct. 2004; Nuclear Science Symposium Conference Record, 2004 IEEE, Volume 1.

[70] The University of Washington group has just joined during these final stages of preparing the proposal, and so is not represented in the budget tables. We will fund the expected (small) travel and M&S costs to support their effort in the alternative substrate and mechanical assembly groups with subcontracts from Argonne.

[71] Argonne National Laboratory, Fermi National Laboratory, Saclay/IRFU, Stanford Linear Accelerator Center, University of Chicago, University of Hawaii; Fermilab Experiment T979; H. Frisch, Spokesperson; Memorandum of Understanding, PSEC Collaboration; Fermilab, Batavia IL; Feb, 2008

[72] MANX project proposal; https://mctf.fnal.gov/meetings/2007-1/04_05/project-narrative-06ER86282-6Manx-v2-w-appendices.pdf/view

[73] C.-M. Kao, Q. Xie, Y. Dong, L. Wan and C.-T. Chen, "Development and Performance Evaluation of a High-Sensitivity Positron Emission Tomography Scanner Dedicated for Small-Animal Imaging" Submitted to IEEE Transaction on Nuclear Science, 2008.

[74] The LHC upgrade is described in: O. Bruning, "LHC challenges and upgrade options", J.Phys.Conf.Ser.110:112002,2008.

[75] M. Diwan, S. Kettell, L. Littenberg, W. Marciano, Z. Parsa, N. Samios, S. White, R. Lanou, W. Leland, K. Lesko, Karsten Heeger, W. Y. Lee, W. Frati, K. Lande, A. K. Mann, R. Van Berg, K. T. McDonald, D. B. Cline, P. Huber, V. Barger, D. Marfatia, T. Kirk, R. Potenza; "Proposal for an Experimental Program in Neutrino Physics and Proton Decay in the Homestake Laboratory"; BNL-76798-2006-IR; arXiv:hep-ex/0608023v2.

[76] H. Frisch, in Photo-Detectors in Water Cherenkov Neutrino Detectors; Workshop, Argonne National Laboratory, Lemont, IL; 20 December 2008; http://www.hep.anl.gov/mcsanchez/large-area-photodet-workshop/

[77] See, for example, D. Acosta et al. (CDF Collaboration); Nucl. Instrum. Meth. A, 2004, pp 605-608

[78] W. Klempt; Nucl. Instrum. Meth. A433: 542-553, 1999; An extensive list of references on timing measurements can also be found in: A. Mantyniemi, MS Thesis, Univ. of Oulu, 2004; ISBN 951-42-7460-I; ISBN 951-42-7460-X; http://herkules.oulu.fi/isbn951427461X/isbn951427461X.pdf

[79] J.L. Wiza, Micro-channel Plate Detectors. Nuclear Instruments and Methods 162, 1979, pp 587-601

[80] S. Cova et al. Constant Fraction Circuits for Picosecond Photon Timing with Micro-channel Plate Photomultipliers. Review of Scientific Instruments, Vol 64-1, 1993, pp 118-124.

[81] T. Credo, H. Frisch, H. Sanders, R. Schroll, and F. Tang; Proceedings of the IEEE, Rome, Italy, Oct. 2004; Nuclear Science Symposium Conference Record, 2004 IEEE, Volume 1.

[82] K. Inami, N. Kishimoto, Y. Enari, M. Nagamine, and T. Ohshima; Nucl. Instrum. Meth. A560, 303-308, 2006

[83] J. Va'vra, J. Benitez, J. Coleman, D. W. G. Leith, G. Mazaher, B. Ratcliff and J. Schwiening, Nucl. Instrum. Meth. A572, 459 (2007)

[84] For a detected photon, a time resolution of 1 psec allows the determination of a spherical shell of thickness ≈1 mm from which the photon originated. The resolution along the beam axis depends on the angle of the photon to the beam, but this will in general allow some confirmation that a photon came from a given vertex.

[85] See, for example, C.H. Chen and J. F. Gunion, Phys. Rev. D 58, 07005 (1998).

[86] T. Aaltonen et al (CDF Collaboration), ArXiv: 0804.1043 [hep-ex], Phys. Rev. D.78.032015 (2008); See also: M. Goncharov, T. Kamon, V. Khotilovich, V. Krutelyov, S.W. Lee, D. Toback, P. Wagner, H. Frisch, H. Sanders, M. Cordelli, F. Habbacher, and S. Miscetti; "The Timing System for the CDF Electromagnetic Calorimeters"; Nucl.Instrum.Meth.A565:538-542,2006;

[87] C.-M. Kao, J. S. Souris, S. Cho; B. C.Penney, C.-T. Chen; Nuclear Science Symposium Conference Record, 2005 IEEE Volume 4, Issue , 23-29 Oct. 2005 Page(s): 2081 - 2084

[88] The DUSEL-specific workshop slides and agenda are available at: http://www.hep.anl.gov/mcsanchez/large-area-photodet-workshop/

[89] We have already achieved the necessary timing resolution in the Fermilab test beam for a 1% momentum resolution for 210 MeV muons in a 10' field-free drift space. The one exception is the possible high magnetic field in the regions of TOF2 and TOF3, depending on the detailed layout.

[90] K.A. Jenkins, A.P. Jose, D.F Heidel; An On-chip Jitter Measurement Circuit with Sub-picosecond Resolution; Proceedings of the 31st European Solid State Circuits Conference, Vol 12, pp 157-160, 2005

[91] Systematic errors in sampling may be calibrated out with the use of extra calibration channels in the front-end readout.

14 Appendix C: Advanced Photo-cathodes

Photocathode Technology for the Near UV – Visible Regime

Alkali photocathodes have been employed for many decades as the principal detection method for visible photon wavelengths in photo multiplier tubes (PMT) (Sommer, 1980) due to their high quantum efficiency (QE) and economical production with high yields. The photocathode is responsible for converting the optical photons to free electrons, which are then accelerated into an amplifying structure to achieve gain. A perfect cathode will show a very high absorption in the spectral range of interest, a high electron yield, low thermal noise, low reflection losses, and fast time response. The optimum photocathode has also to meet a wide variety of engineering, process and materials compatibility, and lifetime requirements. To a large degree these properties will determine the demands on the vacuum system, the complexity of the mechanical detector assembly, and therefore the cost efficiency of the full detection system. The project will have to meet additional challenges by scaling up the production processes to large areas and ensuring the necessary quality control.

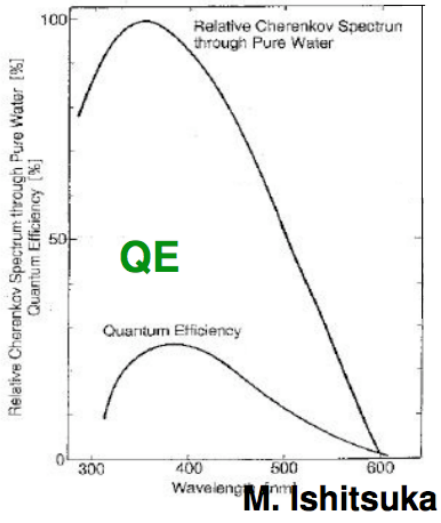

Fig. 1 Cherenkov emission spectrum for pure water, compared with the bialkali photocathode response curve for a Hamamatsu PMT.

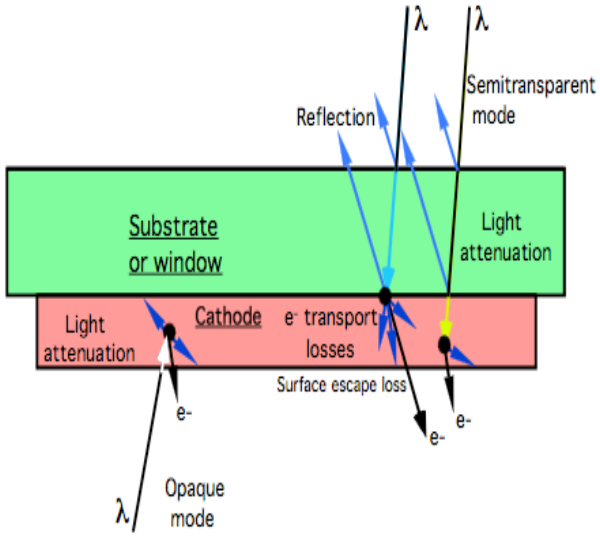

Fig. 2 Schematic of opaque and semitransparent alkali photocathode geometries for optical photon detection.

To convert photons to free electrons the cathode has to provide a high absorption probability for photons, a fast and low loss path for photoelectron(s), and a minimal surface escape barrier for electrons to escape from the surface. Over the years a wide range of materials has been discovered which fulfill these three tasks. Bialkali cathodes (for example Na_2KSb), Multialkali photocathodes ($Na_2KSb(Cs)$), and GaAs type photocathodes with various dopants (P, In) are typical for the near UV, visible and near IR regimes. For alkali photocathodes operating through the simple photoelectric effect, a fraction of the produced primary photoelectrons can leave if their residual kinetic energy is larger than the work function (the energy barrier between the surface state and the free vacuum levels). The lowest photon energy which can be principally detected must be higher than band gap plus the work

function of the cathode material. One substantive difference between cathode types is the noise, expressed in terms of a dark counting rate. Bialkali cathodes are comparatively quiet at room temperature (Fig. 5) (10 to 100 events cm^{-2} sec^{-1}) compared with semiconductor or multialkali cathodes (1000 to 50000 events cm^{-2} sec^{-1}). This means <10,000 events cm^{-2} sec^{-1} for an 8"-square panel using bialkali, versus >4 MHz for a "red" cathode.

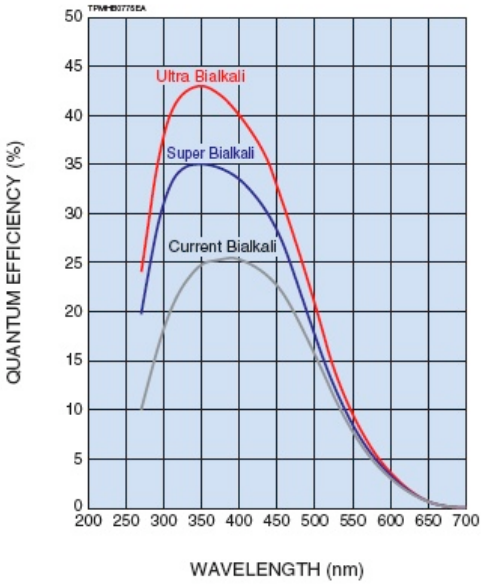

Fig. 3. High efficiency bialkali cathode results from the Hamamatsu catalog.

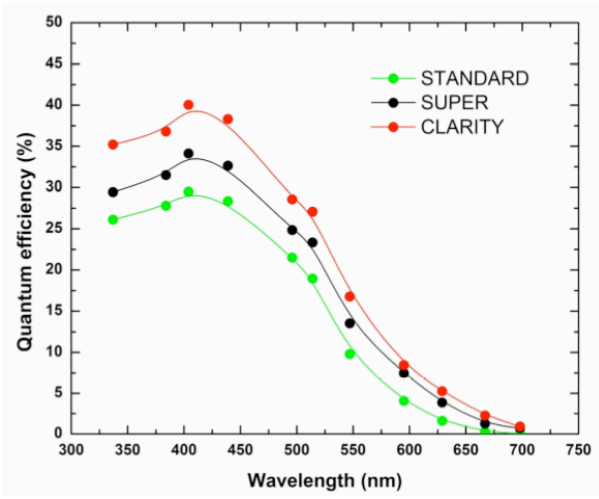

Fig. 4. High efficiency bialkali photocathodes developed by Photonis (Kapusta, et al 2007).

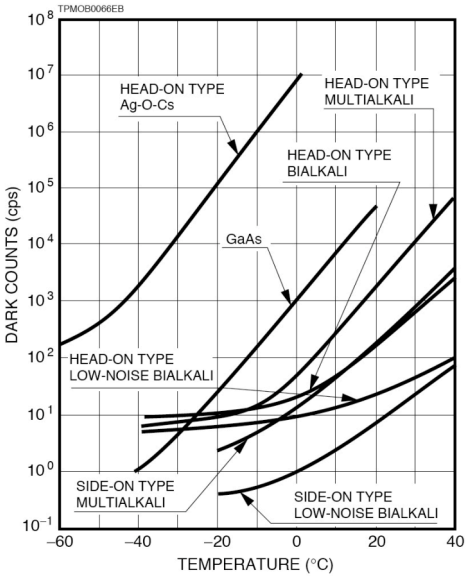

Fig. 5. Background event rates for various photocathode types as a function of temperature.

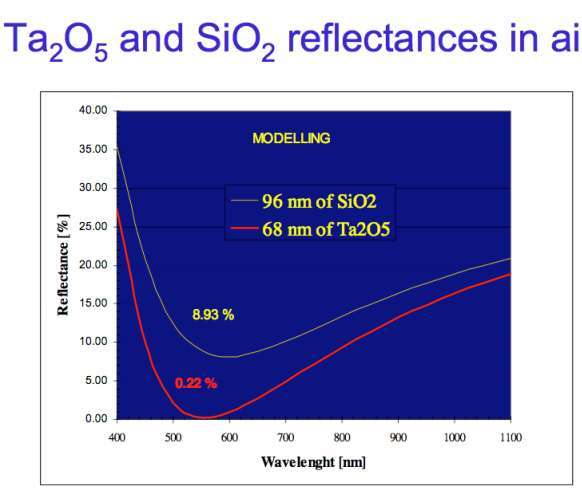

Fig. 6. Effects of anti-reflective coatings on entrance window reflectivity in a water medium, optimized for 530nm light.

The spectrum of Cherenkov light in pure water is shown in Fig. 1. This closely matches the response curve of bialkali photocathodes, which is also shown. Recent state-of-the-art bialkali cathode technology provides at least 20%-25% electron efficiency over the visible spectral range. Present state-of-the-art bialkali cathodes, developed by Photonis and Hamamatsu a few years ago (Mirzoyan et al. 2006), have reached peak levels in excess of 40% (Figs. 3, 4). A combination of recapturing transmitted photons, the optimization of the thickness and composition of the cathode efficiency during the production process, and the use of anti-reflective layers under the cathode (Fig. 6) are responsible for these improvements.[1, 2]

Standard bialkalis fabricated in the Space Science Center (SSL) facilities have similar efficiency (20%) to those that have been traditionally produced. These types of cathode have been made on substrates up to 4" in diameter (Fig. 7, 8). Increasing the size and efficency of bialkali photocathodes in the geometry desired for our project requires somewhat different implementation than used for the Hamamatsu and Photonis PMTs, as a large planar geometry is uniquely different from `tulip' shaped PMT enclosures. A program of optimization, and accommodation can be envisaged which addresses the needs of this program. Small standard size (25mm cathode) and 32.8mm MCP tubes can be employed to establish the correct cathode implementation techniques, and then large test articles can be made to investigate the scale-up issues such as cathode uniformity.

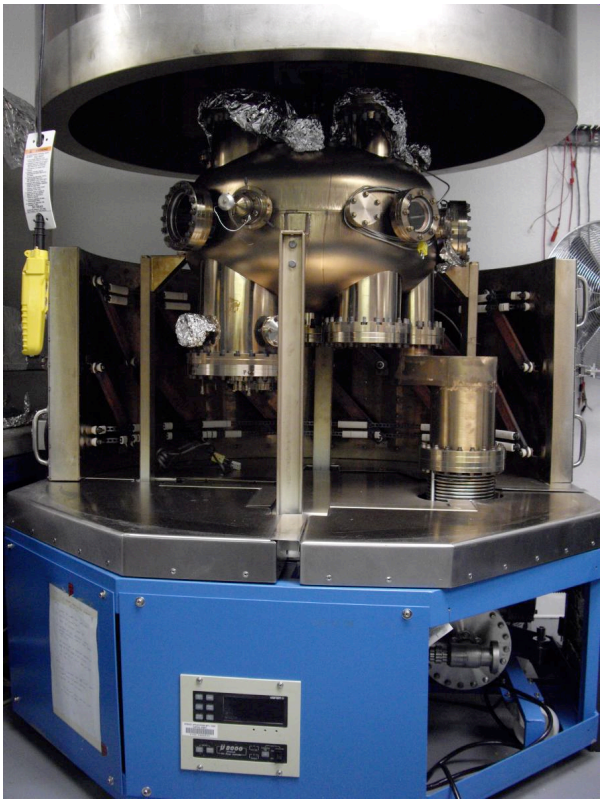

Fig. 7. Large ultrahigh vacuum process tank capable of accommodating 10" photocathodes at SSL.

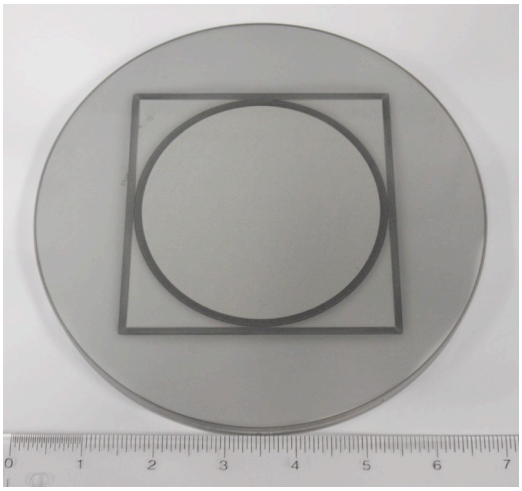

Fig. 8. Large 7" fiber optic used for the entrance window of a bialkali cathode tube.

The choice of the correct input window is part of this process, where borosilicate glass is acceptable but not as good as fused silica for transmission concerns. Application of anti-reflective coatings is extremely important (Fig. 6) to minimize losses over the wavelength

range of interest, and if used under the cathode must be applied before the cathode processing. In situ manipulation of the cathode material deposition follows fairly well defined rules, although optimization of the metals deposition can have substantial effect on the end result. Recapture of transmitted photons requires geometrical design considerations. In our case a flat geometry can be enhanced by the use of highly reflective coatings of electrode material on the top of the MCP, which is directly below the window/cathode. Lastly, attempts were made a number of years ago to deposit bialkali cathodes directly onto MCPs to provide an "opaque" cathode. Opaque cathodes generally have higher efficiencies than semitransparent cathodes because the absorption depth can be made far deeper than the photoelectron emission depth, though use of acute angle surfaces and/or rough surfaces. Normal MCPs are poor substrates as they contain many contaminants. However, the MCP substrates under consideration for this program are chemically inactive. Therefore tests of bialkali photocathodes directly deposited onto the MCP (glass/AAO) surface and down several pore diameters will be investigated. Once these techniques have been investigated in small format geometry, we can apply the results to larger areas and evaluate the efficiency, stability and uniformity of large area (8") substrates and geometries.

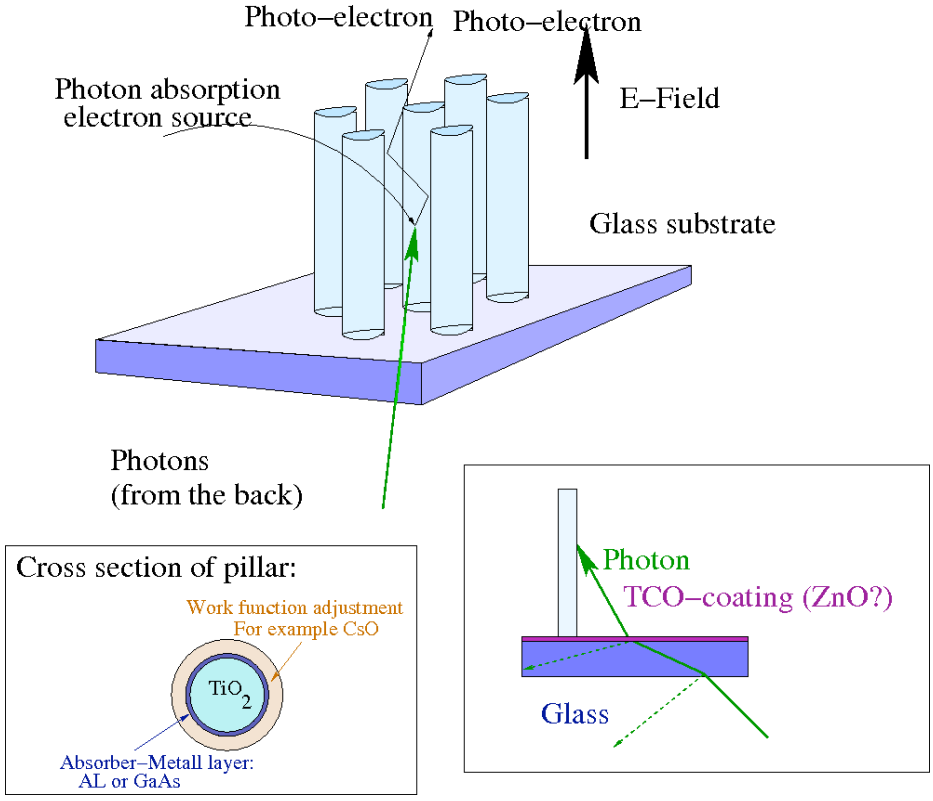

Figure 8: Schematic structure of a morphology-based photo-cathode; the glass substrate (quartz) is coated on one side with a transparent conductive oxide (TCO) which will ensure an equipotential surface. This surface is covered by pillars, each working as an individual NEA-cathode. The structure will act like a photon trap reducing reflection losses and increasing the effective absorption thickness of the cathode.

In parallel to this established route we want to explore a novel photocathode concept based on a nano-structured morphology. This morphology will increase significantly the surface-to-volume ratio, allows a wide range of band-structure engineering tools to optimize noise/efficiency for a given spectral range, reduce optical reflection losses, and to improve the lifetime of the cathode under relaxed vacuum conditions by reducing ion-etching effects.

By changing the cathode from a flat film to a structured morphology such as pillars, the effective thickness of the cathode will be increased and the reflection losses minimized.[3] One example for such new technologies is the so-called "moth-eye" technology developed for solar cells[4] where the insects' eyes are covered by nanostructured coatings. This creates layers in which the refractive index gradually changes from one to the value of the insects' optical nerve. The resulting effect is very little light is reflected out of the eye. This technology can be transferred to cathode technology. In our case the support structure forming the morphology of the cathode should be transparent and slightly p-doped to avoid charging effects. Each pillar is coated with a nearly intrinsic optically dense semiconductor layer 50-100nm thick, which is terminated with 5-10nm of negative electron affinity (NEA) material. The semiconductor structure of the pillar follows a PIN-diode structure, creating a strong radial electric field in the active area of the pillar resulting in effective electron emission. For similar structures field strengths of about 4V/μm are reported.[5] As shown in Figure 8, the light will penetrate the glass substrate from the backside, and hit one of the pillars. Either the photon will be absorbed in the active area and converted in a photoelectron or it penetrates the pillar and will be absorbed on the backside or on a neighboring pillar. We want to emphasize that the photon will be mainly absorbed in active areas since the support structure is transparent. A moderate field perpendicular to the cathode surface (along the pillar main axis) will extract the electrons from the cathode. Preliminary simulations, shown in Figure 9 based on a not-yet-optimized geometry, show that the transient time of the electron through the cathode is insensitive to the emission angle of the electron. Therefore the timing characteristics will be only slightly broadened (by less than 3.5ps for the given simulation). An interesting aspect of this geometry is that the active area of the cathode is not directly exposed to the positive ion bombardment from the MCP channels since the surface is parallel to the electric field lines. Due to the electric field distribution most of the ions will hit the non-active top of the pillars resulting in no damage.

To design the photocathode coating we will utilize knowledge from planar cathode design. The optical absorption layer, for example 300nm GaAs, is combined with a second strongly *n*-doped thin semiconductor layer. This negative electron affinity (NEA) layer has a reduced work function in comparison to the bare absorption layer and, similar to a *pn*-transition of a diode, introduces an electric field perpendicular to the surface.[6, 7] This field breaks the symmetry and creates a force on the thermalized electrons. The carriers are pushed towards the surface, increasing the electron emission.[6] Typically the NEA layer is formed from a Cs-O thin film of about 10nm-50nm. By changing the stoichiometry of Cs and O the defect concentration can be optimized to result in a strongly n-doped film.[8] The optimization process requires an in-situ measurement of the cathode efficiency during the production process.[9] The introduced electric field permits increasing the absorption layer thickness of the cathode. In addition, the oxide layer is insensitive against oxidation. Over a wide spectral range (250nm-700nm) efficiencies of 20%-26% are reported for planar GaAs-CsO cathodes.[10] The bandgap

of the intrinsic-absorption layer can be widely tuned from 0.4eV to nearly 2.2eV by changing the composition of GaAs to $In_xGa_{(1-x)}As$ or $Al_xGa_{(1-x)}As$ compositions. The layer can be built up either homogeneously or in a layered structure to allow optimization for multiple wavelengths. The noise behavior will depend mainly on the bandgap for intrinsic materials. A comparison with Si-PIN detector technology shows that a bandgap of about 1.2eV results in a negligible noise behavior at a temperature of about 0C. In the case of real materials it will mainly depend on defect densities and interface reconstruction effects, which yield to n-doping creating free electrons. This effect can be minimized by growing excellent film structures and by compensation doping, as it is done in PIN-diode and Si-drift detector technology.

The development of the morphology-based NEA-cathode is based on extensive efforts using nano-technology to create cathodes for other applications like solar cells, and light emitting devices. We propose to develop the structures on the basis of TiO_2-nano rods. TiO_2 based materials provide a large variety of morphologies. Various low and high temperature processes have been reported which results in well-defined morphologies on various

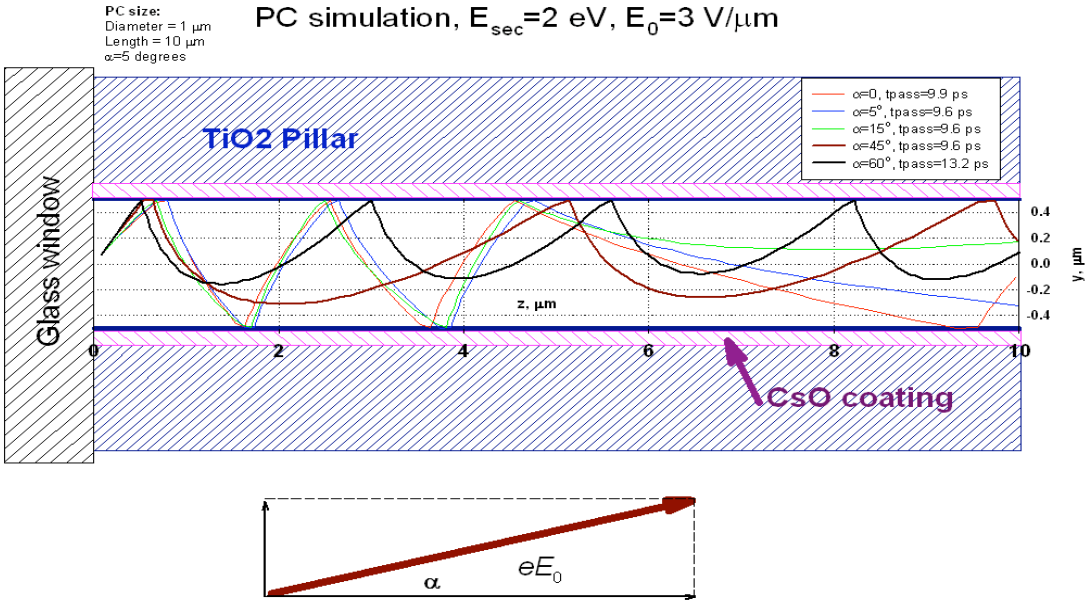

Figure 9: Simulation of the electron path through pillars dependent on various emission angles; the geometry is not optimized. The simulations show that the transient time is insensitive to the emission angle of the electron.

substrates.[11, 12] This material is compatible with atomic layer deposition (ALD) which permits growing a Cr-doped TiO_2 top layer.[13] The ability of coating complex morphologies homogeneously makes ALD an enabling technology. The TiO_2/Cr layer will be p-doped to provide the necessary optical transparence, conductivity to avoid charging effects, and the first layer of the PIN-structure. Alternative p-doped layers may be AlGaAs doped with Si. Multiple variations exist for the growth of the optical absorption and the NEA layer. Following state of the art NEA-flat-cathodes designs, we will use GaAs and CsO layers.[14] We will also explore alternatives such as Ge-based optical absorption layers with Si/Cs/O NEA layers.[15, 16] For highly UV-sensitive cathodes we suggest an Au-CsO combination.[17] All these

layer combinations will be compatible with ALD or similar deposition techniques.[18-21] We want to emphasize that these activities will fully utilize the materials sciences competency of Argonne National Laboratory's Center for Nano-scale Materials, Material Science Division and Electron Microscope Center, as well as the test facilities of the Advanced Photon Source and the computational facilities of the Mathematics and Computer Science Division.

References:

1 M. Kapusta, P. Lavoute, F. Lherbet, et al., 2007 IEEE Nuclear Science Symposium Conference Record, 73 (2007).

2 R. Mirzoyan, M. Laatiaoui, and M. Teshima, Nuclear Instruments & Methods in Physics Research Section a-Accelerators Spectrometers Detectors and Associated Equipment **567**, 230 (2006).

3 W. F. Bogaerts and C. M. Lampert, Journal of Materials Science **18**, 2847 (1983).

4 G. V. Silke L. Diedenhofen, Rienk E. Algra, Alex Hartsuiker, Otto L. Muskens, George Immink, Erik P. A. M. Bakkers, Willem L. Vos, Jaime Gómez Rivas, Advanced Materials **Volume 21**, 973 (2009).

5 J. J. Zou, Z. Yang, L. Qiao, et al., Optoelectronic Materials and Devices Ii **6782**, R7822 (2007).

6 L. N. Dinh, W. McLean, M. A. Schildbach, et al., Physical Review B **59**, 15513 (1999).

7 L. N. Dinh, W. McLean, M. A. Schildbach, et al., Flat-Panel Displays and Sensors - Principles, Materials and Processes. Symposium (Materials Research Society Symposium Proceedings Vol.558)|Flat-Panel Displays and Sensors - Principles, Materials and Processes. Symposium (Materials Research Society Symposium Proceedings Vol.558), 533 (2000).

8 J. S. Huang, Z. Xu, and Y. Yang, Advanced Functional Materials **17**, 1966 (2007).

9 L. Liu, Y. J. Du, B. K. Chang, et al., Applied Optics **45**, 6094 (2006).

10 L. Liu and B. Chang, Advanced Materials and Devices for Sensing and Imaging II **5633**, 339 (2005).

11 X. Chen and S. S. Mao, Chemical Reviews **107**, 2891 (2007).

12 X. B. Chen and S. S. Mao, Journal of Nanoscience and Nanotechnology **6**, 906 (2006).

13 G. H. Takaoka, T. Nose, and M. Kawashita, Vacuum **83**, 679 (2008).

14 B. K. Chang, W. L. Liu, R. G. Fu, et al., Apoc 2001: Asia-Pacific Optical and Wireless Communications: Optoelectronics, Materials, and Devices for Communications **4580**, 632 (2001).

15 J. X. Wu, M. S. Ma, J. S. Zhu, et al., Applied Surface Science **173**, 8 (2001).

16 Goldstei.B and Martinel.Ru, Journal of Applied Physics **44**, 4244 (1973).

17 H. Jinsong, X. Zheng, and Y. Yang, Advanced Functional Materials, 1966 (2007).

18 H. Kim, S. Sohn, D. Jung, et al., Organic Electronics **9**, 1140 (2008).

19 S. Won, S. Go, W. Lee, et al., Metals and Materials International **14**, 759 (2008).

20 H. Kim, H. B. R. Lee, and W. J. Maeng, Thin Solid Films **517**, 2563 (2009).

21 A. I. Persson, B. J. Ohlsson, S. Jeppesen, et al., Journal of Crystal Growth **272**, 167 (2004).

15 Appendix D: Anodized Aluminum Oxide Plates

15 Appendix D: Anodized Aluminum Oxide Plates

15.1. Introduction

A microchannel plate (MCP) is a solid-state electron amplifier that contains an array of micropores (channels) typically imbedded in a lead silicate glass. The surface is chemically treated to enhance secondary electron emission from the walls of the channels.[1] A typical commercially available MCP is built with a channel diameter between 6 and 25 microns, and a channel aspect ratio, i.e. the ratio of length to diameter, between 40 and 100 . The smallest channel diameter of which we are aware in a commercial MCP has a channel diameter of 2.3 microns, as shown in Figure 1a.[2]

The typical lead glass MCP is fabricated through a multi-step process starting with melting of new glass materials, fiber drawing , slicing, polishing, and chemical processing.[2] It is elaborate and expensive, and does not seem suited to scaling up for large-area detection applications. New approaches to MCP fabrication that bypass the limitations of glass technologies and enable scalable low-cost manufacturing of larger-area MCPs with high spatial/temporal resolution and improved lifetime are needed.

Nanoporous anodic aluminum oxide (AAO) has been identified as a possible alternative for glass as the substrate for MCPs, due to its similar hexagonally close packed arrays of cylindrical and uniform pores that are perpendicular to the surface (Figure 1b). The diameter of the pores in typical AAO fabrication can be controlled in the range from ~10 nm to ~ 250 nm, with corresponding pore-to-pore spacing from 30 to 600 nm. Contrary to glass MCPs, AAO can be prepared in a simple wet chemistry process, attracted further interest as a candidate for new MCP design and development.

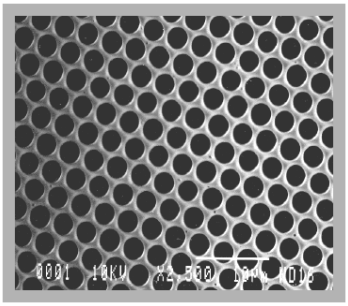

Figure 1a. 2.3 microns commercial MCP from Burle Electro-Optics.

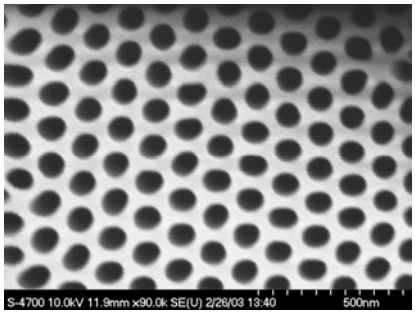

Figure 1b. SEM image of an AAO template with 80 nm pore diameter and 143 nm pore-to-pore distance

AAO has been used as a protective layer over aluminum surfaces in very large scale applications for corrosion prevention as well as metal finishing and decoration. Due to the interest from the areas of nanoscience and technology, starting in 1990-s AAO has been recognized and widely used as templates for nanoscale material synthesis [3-9] In addition, the control of AAO nanostructures has reached a new level recently.[10] Synkera has been using AAO extensively as a nano/microfabrication platform for the development of a variety of products, from membranes for gas separation and nano/ultrafiltration to gas microsensors, BioMEMS and energy conversion materials [11] and has significant related experience.

Although the promise of using AAO for MCP development was recognized in the late 1960-s [12] and further explored in the 1990-s [13], it has not been fully implemented for a number of reasons. ***First***, the typical AAO pore diameter (10 to 250 nm) is too small for creating functional MCPs: (i)

in channels <0.5 μm, the space charge would be excessive for achieving the required gain and high local count rate, (ii) in small pores the electron path is too short to acquire the energy sufficient for secondary electron generation. ***Second***, even for 250 nm channels, the MCP would have to be thin for common aspect ratios and thus unable to withstand the required voltage and too fragile. ***And finally***, no reproducible and controllable processes for uniform modification of the resistance and secondary emission properties were available for high aspect ratio nanopores.

15.2. Challenges in realizing large area low cost MCPs from AAO

The general challenges in realizing large area MCPs for targeted large-area, low-cost detectors are:

- Scaling substrate to large sizes in a batch process to keep the cost down
- Achieving a channel diameter in the range where adequate amplification occurs
- Enabling processing temperatures up to 900°C if photocathodes are to be integrated directly onto the MCP surface

Although several alternative technologies could be considered for this task (including capillary-based glass substrates, porous Si-based, microsphere, and fiber mat plates, etc), using intrinsic pores of AAO is highly attractive due to a number of inherent advantages, such as low cost, scalability, uniformity and thermal range. However, for AAO to be the substrate of choice for functional large area ceramic MCPs, several specific challenges listed below have to be addressed with our approaches outlined in parentheses.

- Developing AAO with a pore diameter ≥ 0.5 μm. (The largest pore diameter demonstrated in the open literature is 250 nm; Synkera has demonstrated feasibility of 0.4 - 0.6 μm channels in small prototypes. New electrolytes and anodization methods need to be developed for achieving larger diameters).
- Retaining a channel structure satisfactory for electron amplification and minimized spontaneous field emission. (Increasing pore size often leads to a heavily distorted and convoluted network of pores. Surface patterning demonstrated by ANL, and stable anodization regimes under development at Synkera could be used to alleviate this issue).
- Maximizing the open area ratio and achieving a funnel shape to maximize the efficiency of the first strike. (Controlled anodization and etching approaches).
- Realizing required channel resistance and secondary emission coefficient. (ALD was confirmed to be the method of choice, Section 14 appendix E).
- Scaling the processes involved in large pore formation to the required size (8”x8”). (Scale-up of the AAO with large pores is far from trivial; issues of uniform current density distribution, heat dissipation and others will be addressed).
- Achieving mechanical integrity in the scaled 8”x8” size for a given MCP thickness. (Will require proper support in the detector body; an Al rim and internal frame structure could be used).
- Demonstrating targeted cost saving

While there are significant challenges remaining in the development of AAO-based MCPs, if realized, it would represent a technical breakthrough and a significant market opportunity for a new generation of large-area ceramic MCPs at a cost below that of other methods.

15.3. Current Status

Conventional AAO has been prepared in sulfuric acid (10-30 nm pores), oxalic acid (40-100 nm pores), and phosphoric acid (larger than 100 nm pores). These pore diameters are one to two orders of magnitude smaller than those of the current MCP. In order not to deviate too much away from a region of the channel sizes that is known to be working very well in MCPs, we plan to bring the AAO pore size closer to the micron and sub-micron region. The prior work related to overcoming the challenges in achieving required AAO channel dimensions, ordered structure and scale, is described in the following subsections.

15.3.1. The bottom-up approach to achieve large Pore Sizes

In order to prepare pores in the 100 to 500 nm region, we will take the hard anodization approach recently reported in the literature.[10] Although the method has been used in industry for surface coating, it is not common in the research community. The reason is that the pore structure is not well-ordered and is difficult to control. This method utilizes a DC anodization potential between 110 and 160 V. Temperature control during anodization is very important to avoid melt-down of the Al surface. Using this approach (hard anodization), ANL has shown a highly ordered pore array with a pore diameter of 240 nm and a pore distance of 350 nm and have successfully prepared an 1" diameter AAO membrane (Figure 2).

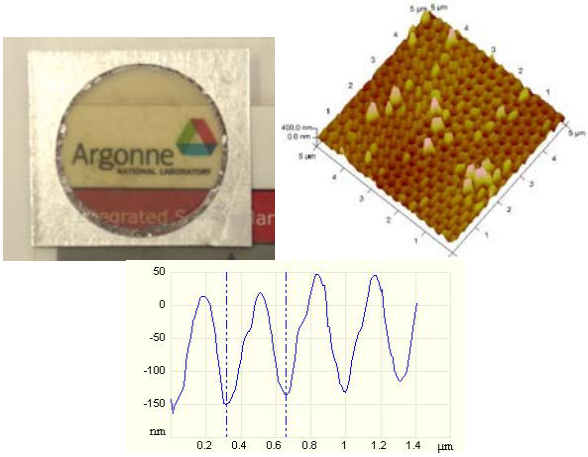

Figure 2. AAO after second anodization at 140 V with Al removed: photograph (left), AFM image of 5x5 μ^2 scan (right), and pore size measurements (bottom).

We plan to utilize our newly explored methods to design and develop new AAO based microchannel plates with larger (0.5-1 µm) pores. To address the challenge of the large pore size for the application of AAO for MCPs, Synkera has been developing new anodization electrolytes and anodization methods that allow significantly expanded boundaries of AAO pore dimensions. To date, Synkera has demonstrated feasibility of channels with diameter up to 0.5-0.6 µm and pore-to-pore distance as high as 1.2 µm (Figure 3a, left). The surface of this AAO has a cone-shaped entrance, a 'funnel' , which when enhanced by chemical etching, can be exploited to create a surface that would increase the efficiency of the "first strike". AAO of this type withstands processing temperatures up to 1100°C without loss of integrity and is being used for the development of the preliminary prototypes of 25 mm MCPs.

15.3.2. AAO Scale-Up

In related prior work on AAO-based gas separation membranes, Synkera successfully scaled the processes and produced free-standing AAO membranes with active areas as large as 8" x 14", on an Al rim (11"x18") for mechanical support (Figure 3b). We will use this relevant AAO scale-up approach and experience to scale the large-pore anodization processes to support the fabrication of scaled 8"x8" MCP substrates.

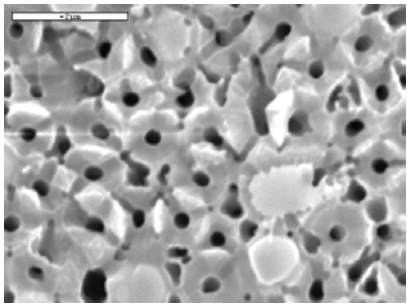

Figure 3a. Surface view of the AAO with pore diameter in the 0.4–0.6 μm range (Synkera). Note the funnels surrounding each pore opening (the circular areas covering most of the surface).

Figure 3b. The world largest AAO membrane (with conventional pores) supported on an Al rim, produced at Synkera Technologies Inc.

15.3.3. Pore Ordering

To complement the bottom-up approach and to reach required pore ordering with a pore-to-pore distance in the 0.5-5 micron region, we propose to combine novel anodization processes that intrinsically support a large pore period, with patterning of the surface of Al to guide the pore initiation process. Pore ordering in AAOs is desirable because device testing results may be readily compared with that from simulation.

We have access to sophisticated facilities that allow exploration of pore ordering. The 2-10 micron pore diameter is where the current MCP operates, and it will be useful to get into this region so that in-depth comparison between porous lead silicate and ALD coated AAO membranes can be done. The following techniques for surface patterning are available to us at the Argonne Center for Nanoscale Materials (CNM): 1) Focused ion beam (FIB), 2) Photolithography, 3) Laser writer, 4) Nanoimprint and indentation techniques. These methods are briefly discussed here.

1) The FIB is a patterning tool. One can generate nearly any patterns in three-dimensions. A hexagonally closed packed (hcp) pattern has been generated over Al (Figures 4a and b) with use of FIB to drill holes on the surface. These holes on the surface will then be used to develop pores through anodization with pore-to-pore distance at exactly 0.5 micron. The pattern is perfect but the main drawback is that FIB is a serial technique and it is expensive and time consuming for a large area. However, for a small area (cm^2), this is a perfect tool for making a prototype for initial testing and proof of concept experiment.

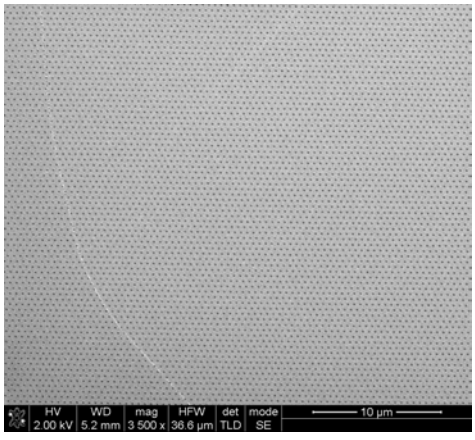

Figure 4a. hcp pattern fabricated at ANL/CNM over Al with use of FIB, 10 μm scale bar.

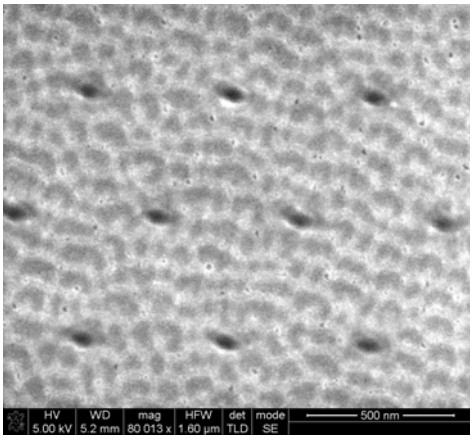

Figure 4b. Same hcp pattern over Al showing 500 nm pore distance, 500 nm scale bar.

2) Photolithography. This is a very good

tool for large areas. To prepare the desired pattern, one needs to first develop a photomask. For large scale applications, once the desired pattern is set, this technique will be very useful.
3) Laser writer. This is a fast prototyping tool. No photomask is needed. One can generate a set of patterns with variable parameters quickly. For our current exploratory research, the laser writer is a useful tool.
4) Nanoindentation. We will first generate a set of patterns with use of a laser writer. After developing the pattern, the features can be coated with a layer of ultra-nano-crystalline diamond (UNCD) to prepare a hardened stamp. The pattern can be repeated over a large area with such a stamp. Other bottom-up approaches, such as nanosphere imprint [14], could be also used for this purpose. The textured surface will then be anodized in the conditions that match the pore period of the pattern to fabricate the desired pore structure. We have all these top-down fabrication processes available to us. In addition to the use of a single piece of equipment, new processes will be developed to utilize several techniques together in order to achieve the goal of making large area detectors.

15.3.4. Pore shape design and development

According to simulation, a funnel shaped pore opening is beneficial to enhance the initial photoconversion and secondary electron emission. Work along this direction has not been reported in the literature. The desired pore configuration for this proposed work is a funnel shaped opening followed with a narrow straight pore. It should be noted that the pore opening in AAO has naturally conical shape, especially if pre-anodization step described above was used to pre-organize the pore lattice. This shape could be further enhanced during the pore widening by chemical etching. Thus, early in the project we will further explore this effect in order to form the desired surface topology. Additional approaches to pore shaping can be explored as well, if needed.

References

[1] J.L. Wiza, "Microchannel plate detectors", *Nuclear Instruments and Methods*, *162* 587-601 **1979**.

[2] B. Laprade and R. Starcher, "The 2 micron pore microchannel plate development of the world's fastest detector", **2001**, http://www.burle.com/cgi-bin/byteserver.pl/pdf/2micron2.pdf

[3] D. Routkevitch, T. Bigioni, M. Moskovits, J. M. Xu, Electrochemical Fabrication of CdS Nano-Wire Arrays in Porous Anodic Aluminum Oxide Templates, *J. Phys. Chem*., *100*(33), 14037-14047 **1996**.

[4] D.Routkevich, A. Tager, J. Haruyama, D. Al-Mawlawi, M. Moskovits and J. M. Xu, Nonlithographic Nanowire Arrays: Fabrication, Physics and Device Applications, Special Issue of *IEEE Trans. Electron Dev.* on "Present and Future Trends in Device Science and Technologies", *43*(10), 1646-1658 **1996**.

[5] Z. L. Xiao, C. Y. Han, U. Welp, H. H. Wang, W. K. Kwok, G. A. Willing, J. M. Hiller, R. E. Cook, D. J. Miller, G. W. Crabtree, "Fabrication of Alumina Nanotubes and Nanowires by Etching Porous Alumina Membranes", *Nanoletters* 2(11), 1293-1297, **2002**.

[6] H.H. Wang, C.Y. Han, G.A. Willing, Z. Xiao, "Nanowire and Nanotube Syntheses Through Self-assembled nanoporous AAO Templates", *Mat. Res. Soc. Symp. Proc.*, *775*, 107, **2003**.

[7] C.Y. Han, Z.L. Xiao, H.H. Wang, G.A. Willing, U. Geiser, U. Welp, W.K. Kwok, S.D. Bader, G.W. Crabtree, "Porous anodic aluminum oxide membranes for nanofabrication" *ATB Metallurgie*, *43*, 123, **2003**.

[8] G. Xiong, J. W. Elam, H. Feng, C. Y. Han, H.-H. Wang, L. E. Iton, L. A. Curtiss, M. J. Pellin, M. Kung, H. Kung, P. C. Stair, "Effect of Atomic Layer Deposition Coatings on the Surface Structure of Anodic Aluminum Oxide Membranes", *J. Phys. Chem.B*. *109*, 14059-14063, **2005**.

[9] C.Y. Han, G.A. Willing, Z. Xiao, and H.H. Wang, "Control of the Anodic Aluminum Oxide Barrier Layer Opening Process by Wet Chemical Etching", *Langmuir 23,* 1564-1568 **2007**.

[10] W. Lee, R. Ji, U. Gösele, and K. Nielsch, "Fast fabrication of long-range ordered porous alumina membranes by hard anodization", *Nat. Mater.* 5, 741-747, **2006**.

[11] See http://www.synkera.com, including links to "Self-organized Anodic Aluminum Oxide" and "Ceramic MEMS" sections; also A. Govyadinov, P. Mardilovich, D. Routkevitch, et al, Anodic Alumina MEMS: Applications and devices, Microelectromechanical Systems (MEMS) 2000, *Proc. ASME Int. Mech. Eng. Congress*, Nov. 5-10, 2000, Orlando, Florida, Vol. 2, ASME, New York, 313-318 **2000**.

[12] US Patents ## 362633, 3724066, 3760216.

[13] A. Govyadinov et. al., *Nucl. Instr. Methods Phys. Res.*, A 419, 667-675 **1998**; F. Emel'yanchik, A. Govyadinov et al., *Appl. Surf. Sci*., ,*111*, 295-301 **1997**.

[14] S. Fournier-Bidoz, V. Kitaev, D. Routkevitch, I. Manners, G. A. Ozin, Highly Ordered Nanosphere Imprinted Nanoporous Anodic Alumina (NINA), *Adv. Mater., 16* (23-24), 2193-2196 **2004**.